A Procedure for the Improved Continuous Stress Field of Composite Media

Kee-Nam Song*

(Received December 2, 1997)

Interfacial tractions at the interface of two different materials and the initial displacement field over the entire domain are obtained by modifying the potential energy functional with a penalty function, which enforces continuity of the stresses at the interface of two different materials. Based on the initial displacement field and the interfacial tractions, a method to build a continuous stress field over the entire domain has been proposed by combining the modified projection method for the stress-smoothing and the Loubignac-Cantin iteration for the restoration of momentum balance in the smoothed stress fields. Stress analysis is carried out on two examples made of highly dissimilar materials. Results of the analysis show that the proposed method provides an improved continuous stress field over the entire domain, and accurately predicts the nodal stresses at the interface of two different materials. In contrast, the conventional displacement-based finite element method produces significant stress discontinuities at the interface of two different materials. In addition, the total strain energy evaluated from the improved continuous stress field rapidly converges to the exact solution as the number of iterations increases.

Key Words : Displacement-based Finite Element Method, Dissimilar Material, Penalty Function Method, Stress Smoothing Method, Conjugate Stress, Interface Traction

1. Introduction

Media consisting of different materials are becoming increasingly common in engineering structures. Examples include thermostats for measuring temperature, metallic parts of etched silicon bases of microchips, attachments between prosthetic materials and biological tissues in orthopedic biomechanics, heat-resistant materials in aerospace vehicles, and the zirconium-lined cladding tubes of nuclear fuel rods. In such non-homogeneous composites, accurate evaluation of the stresses at the interfaces between dissimilar materials are usually of significant importance in both their analysis and design (Shirazi-Adl, 1992; Kim and Lee, 1994; Kim, 1994). To ensure a perfect bond, the computed interfacial stresses should not exceed the bond strength; otherwise separation may occur, which could completely change the displacements and stresses, requiring re-analysis with updated interface conditions. Assuming a perfect bond at the interface, i. e., no separation or slip at the interface, the in-plane tangential strain must be continuous, while the normal and shear strains may be discontinuous. The stress boundary conditions at the interface are determined from the required continuity of the traction vector. That is, in contrast to the strain components, the normal and shear stress components are required to be continuous, while the tangential component should be discontinuous.

In the displacement-based finite element method, the displacements are the primary unknowns of the analysis, and are usually taken to be continuous to the degree that the functional of the problem requires. The stresses in each element are then evaluated based on the displacements and constitutive relations. However, such a consistent procedure results in stresses that are incom-

* Korea Atomic Energy Research Institute, 150 Dukjin-dong, Yuseong-go, Taejon 305-353, Korea

patible at the interface between adjacent elements. To overcome this shortcoming, several suggested procedures have been proved to be effective in the analysis of homogeneous media because of the small discrepancies in inter-element stresses reported in the literature(Brauchli and Oden, 1971; Hinton and Campbell, 1974; Loubignac, Cantin, and Touzot, 1985; Zienkiewicz and Zhu, 1992). Zienkiewicz, Li, and Nakazawa(1985) proved that combining the projection method for stress-smoothing and the Loubignac-Cantin iteration for the restoration of momentum balance in the smoothed stress fields was identical to the mixed formulation when full convergence was reached. In addition, Zienkiewicz *et al.*(1985) showed that the combining of the projection method and the Loubignac-Cantin iteration could effectively solve a mixed stress-displacement formulation of elasticity problems. However, those procedures are primarily of a post-processing nature, and are based on computed nodal displacements. Since the stress incompatibility becomes evident, especially at the interface of two different materials, even for the stress components which must be continuous, the foregoing post-processing methods which were proposed to overcome a violation of the inter-element equilibrium are not suitable in the analysis of non-homogeneous media. In particular, the foregoing post-processing methods may result in severe oscillations of the solution at the interface of two different materials.

Recently, research to find the stress field at two material interfaces has been carried out. Shirazi-Adl(1989, 1992) proposed that a penalty function be added to the usual potential energy functional. The penalty function enforces the compatibility of traction on the element interfaces of two different materials. The modified functional is minimized and the equations generated are solved in the conventional manner. The stresses are then calculated from the predicted nodal displacements using strain-displacement relations and constitutive equations. This formulation results in no extra degrees of freedom but the structural bandwidth may increase. Chouchaoui and Shirazi-Adl (1992) and Kim and Lee(1994) proposed mixed variational formulations based on the Hellinger-Reissner theorem, and Kim(1994) proposed a perturbed Lagrangian method for the 2-D dissimilar bonding problem.

In this study, the initial displacement field over the entire domain and the interfacial tractions at the interface of two different materials are obtained by modifying the potential energy functional with a penalty function. The interfacial tractions at the interface of two different materials are imposed as the constraints in the projection method for stress smoothing. New displacement fields and displacement-consistent stress fields are then obtained by combining the modified projection method with Loubignac-Cantin iteration. Stress analysis is carried out on two examples made of highly dissimilar materials.

2. Finite Element Formulation

Figure 1 shows the domain consisting of dissimilar materials. Assuming a perfect bond at the interface of two different materials, the constraint equations of the interface tractions may be written as:

$$T_i^a + T_i^b = 0 \tag{1}$$

where superscripts a and b denote the material sides of the interface of two different materials, and subscript i varies from 1 to 3 in a three-dimensional analysis. This equation can be regarded as the Euler equation of the conventional potential energy functional. The usual potential energy, π_p, may be modified by imposing the constraint Eq. (1) as a penalty term:

$$\pi_p^* = \pi_p - \frac{1}{2}\alpha \int_S (T_i^a + T_i^b)^2 dS \tag{2}$$

where α is a penalty number and S represents the common interface surface. The first term on the right-hand side results in the well-known element equations and is not discussed further. In the

Fig. 1 Interface traction acting on a bi-metallic interface between two region a and b.

second penalty term, T_i^a and T_i^b may be expressed as vectors by:

$$\{T^a\}=[n^a][E^a][B^a]\ \{d^a\} \tag{3}$$

$$\{T^b\}=[n^b][E^b][B^b]\{d^b\} \tag{4}$$

where $[n]$ is the matrix of the directional cosines of the unit outward vector normal to the interface S; $[E]$ is the elasticity matrix; $[B]$ is the strain-displacement matrix; and $\{d\}$ is the column vector of the element nodal displacements. Combining the two adjacent interface elements into one with $\{d^{ab}\}$ as the column vector of displacements, we obtain:

$$\{T^a+T^b\}=[K^{ab}]\{d^{ab}\} \tag{5}$$

where

$$[K^{ab}]=[n^a]([E^a][B^a][T^a] - [E^b][B^b][T^b]) \tag{6}$$

and $[T^a]$ and $[T^b]$ are the transformation matrices. Finally, the symmetric stiffness matrix for the interface of two different materials due to the penalty function is:

$$[K_p]=\int_S [K^{ab}]^T\ [K^{ab}]\,dS \tag{7}$$

which should be added to the conventional stiffness matrix, $[K]$. *i. e.*,

$$[K^*]=[K]+\alpha[K_p] \tag{8}$$

Then, the system equations become:

$$[K^*]\{u\}=\{f\} \tag{9}$$

where $\{u\}$ is the column vector of nodal displacement components for the entire domain and $\{f\}$ the column vector of the resultant nodal forces.

The terms in the interface penalty matrix $[K_p]$ are noted to be larger than those in the conventional stiffness matrix, the difference being of the same order as that of the moduli. Considering the difference in the order of the moduli, therefore, an appropriate penalty can be selected in the formulation.

3. Build-up of the Continuous Generalized-stress Field

Assuming that the stress field maintains C° continuity, the stress field, $\{\sigma^*\}$, is expressed as a linear combination of the nodal stress vector, $\{\bar{\sigma}^*\}$, and the shape function vector, $[N^*]$, as follows:

$$\{\sigma^*\}=[N^*]\{\bar{\sigma}^*\} \tag{10}$$

Usually in the analysis of homogeneous media, the nodal stress vector, $\{\bar{\sigma}^*\}$, can be obtained by the following projection method (Zienkiewicz, Li, and Nakazawa, 1985) of the discontinuous stress field, $\{\sigma\}$, from the conventional finite element method in the mean sense:

$$I=\int_\Omega [N^*]^T(\{\sigma^*\}-\{\sigma\})\,d\Omega=0 \tag{11}$$

Results from Eq. (11) in the analysis of non-homogeneous media, however, provide not only inappropriate stress fields over the entire domain, but also inaccurate interfacial tractons at the interface of two different materials.

At the interface of two different materials, therefore, the stress field should be the same as the interface tractions, $\{\sigma_{sp}\}$, which are obtained from the penalty finite element formulation of Sec. 2:

$$\{\sigma^*\}=\{\sigma_{sp}\} \tag{12}$$

In order to build a stress field (i. e., the field composed of continuous stress and strain components at the interface) over the entire domain which satisfy the interface tractions, the functional (11) may be modified by imposing the specified tractions of Eq. (12) as follows (Song, 1997):

$$I^*=I+\alpha_\sigma\int_S [N^*]^T(\{\sigma^*\}-\{\sigma_{sp}\})\,dS=0 \tag{13}$$

where α_σ is a penalty number and S represents the common interface surface. Re-arranging Eq. (13) with respect to $\{\bar{\sigma}^*\}$ yields the following:

$$\{\bar{\sigma}^*\}\left(\int_\Omega [N^*]^T[N^*]\,d\Omega+\alpha_\sigma\int_S [N^*]^T[N^*]\,dS\right) = \int_\Omega [N^*]^T\{\sigma\}\,d\Omega+\alpha_\sigma\int_S [N^*]^T\{\sigma_{st}\}\,dS \tag{14}$$

Solving Eq. (14) for $\{\bar{\sigma}^*\}$, the continuous stress field over the entire domain satisfying the specified tractions at the interface of two different materials is obtained from Eq. (10).

4. Iterative Method

The nodal force vector, $\{f^*\}$, due to a continuous stress field, $\{\sigma^*\}$, is obtained by the following equilibrium equations:

$$\int_{\Omega}[B]^{*T}\{\sigma^*\}d\Omega=\{f^*\} \tag{15}$$

where $[B]^*$ denotes a generalized strain-displacement matrix defined as follows:

$[B]^*=[B]$ for continuous stress components, and

$[B]^*=[E][B]$ for continuous strain components.

Since the nodal force vector, $\{f^*\}$, does not equal the force, $\{f\}$, from the original finite element equilibrium, a new displacement field is built by the following iterative algorithm. While Loubignac, Cantin, and Touzot (1977) used simple nodal averaging to obtain $\{\sigma^*\}$, which could be inaccurate at the interface of two different materials, a continuous stress field obtained from the procedure in Sec. 3 is used.

i) $$\{\Delta u\}^i=[K]^{-1}(\{f\} - \sum_{elenemt}\int_{\Omega}[B]^{*T}\{\sigma^*\}d\Omega_e) \tag{16}$$

ii) Compute the nodal force vector that corresponds to the stress, σ^*

$$f_e=\int_{\Omega}[B]^T\sigma^*d\Omega_e=\int_{\Omega e}[B]^TN_i^*d\Omega_e\bar{\sigma}^* \tag{17}$$

$$f^*=\sum_{elenemt}f_e=\sum_{elenemt}\int_{\Omega e}[B]^T\sigma^*d\Omega_e = \sum_{elenemt}\int_{\Omega e}[B]^TN_i^*d\Omega_e\bar{\sigma}^* \tag{18}$$

and the L_2-norm of force-imbalance, $\|\triangle f\|_i$ at the i-th iteration is defined as follows:

$$\|\Delta f\|_i^2=\int_{\Omega}(f-f_e)^T(f-f_e)\,d\Omega \tag{19}$$

iii) $$\{u\}^{i+1}=\{u\}^i+\{\Delta u\}^i,\ i=1,2,3,\cdots \tag{20}$$

iv) $$\{\sigma\}^{i+1}=[E][B]^*\{u\}^{i+1} \tag{21}$$

v) Build a new continuous stress field using the procedure in Sec. 3.

vi) Go to step i) unless the L_2-norm of the perturbed displacement, $\|\Delta u\|^i$ is less than a preset value.

In this study, 1.0E-03 is used as the preset value of $\|\Delta u\|^i$.

The Total strain energy (U_{total}) from the continuous stress field is obtained as follows:

$$U_{total}=\frac{1}{2}\int_V\sigma^{*T}\varepsilon^*dV=\frac{1}{2}\int_V\sigma^{*T}E^{-1}\sigma^*dV \tag{22}$$

where ε^* denotes the strain in the domain.

5. Numerical Examples

5.1 Example 1: Two-material cantilever beam under end load

Figure 2 shows a cantilever beam composed of two highly dissimilar materials, in which the elastic modulus of one material is a hundred times as large as that of the other, and shows its finite element model with quadrilateral plane stress elements. The end forces are computed and applied in a manner consistent with the quadratic variation of end shear stresses in each material region evaluated based on the analytical solution (Muskhelishvili, 1963, pp. 641~649). The results for the penalty formulation are based on $\alpha=0$, $\alpha_\sigma=10000$, and one-point integration. The analytical solution is compared with the conventional displacement-based finite element solution (ANSYS results) and the present results. The variation of the stresses at the interface of two different materials along the beam is shown in

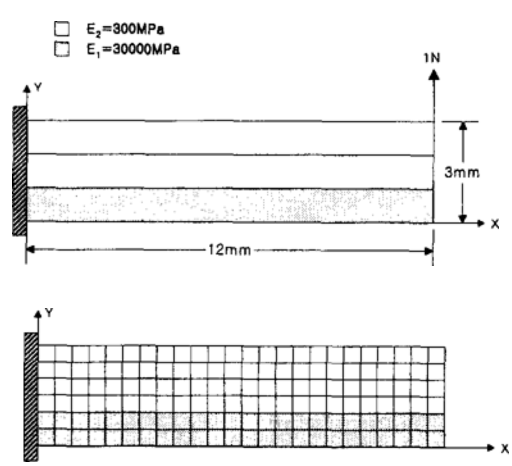

Fig. 2 A two-material cantilever beam under end load.

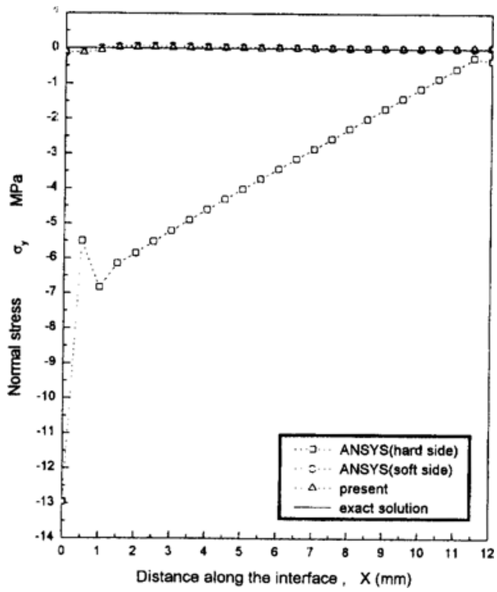

Fig. 3 Variation of the normal stress at the two-material interface along the cantilever beam ($E_1/E_2=100$).

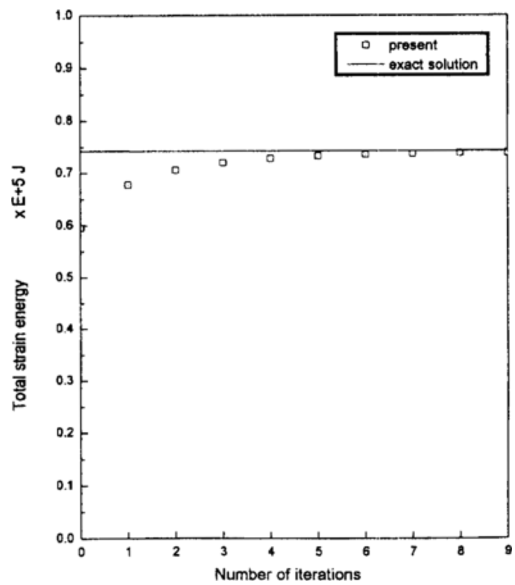

Fig. 5 Total strain energy vs. iteration numbers for the two-material cantilever beam ($E_1/E_2=100$).

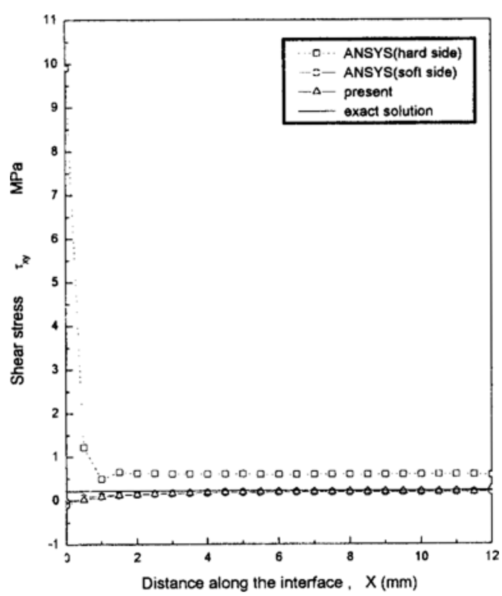

Fig. 4 Variation of the shear stress at the two-material interface along the cantilever beam ($E_1/E_2=100$).

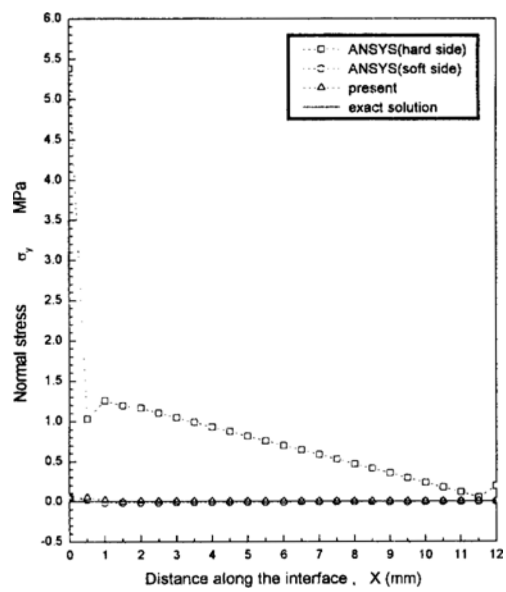

Fig. 6 Variation of the normal stress at the two-material interface along the cantilever beam ($E_1/E_2=0.01$)

Figs. 3 and 4. Comparison of the results of the conventional finite element analysis reveals a very significant discontinuity between the computed stresses on the hard and soft sides of the interface. However, the present method yields nearly identical stresses in both materials at the interface. In addition, both stresses from the present method and the conventional finite element stresses on the soft side of the interface are in agreement with the exact results ($\sigma_y=0$, $\tau_{xy}=0.21929$ MPa) in every area except the region close to the fixed end. The variation in total strain energy calculated from Eq. (22) as iteration numbers is shown in Fig. 5. Total strain energy at the 0-th iteration denotes a value from the conventional averaged stress field.

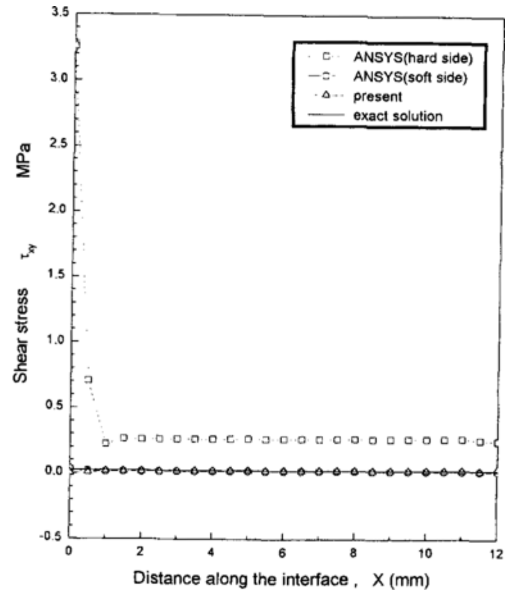

Fig. 7 Variation of the shear stress at the two-material interface along the cantilever beam ($E_1/E_2=0.01$)

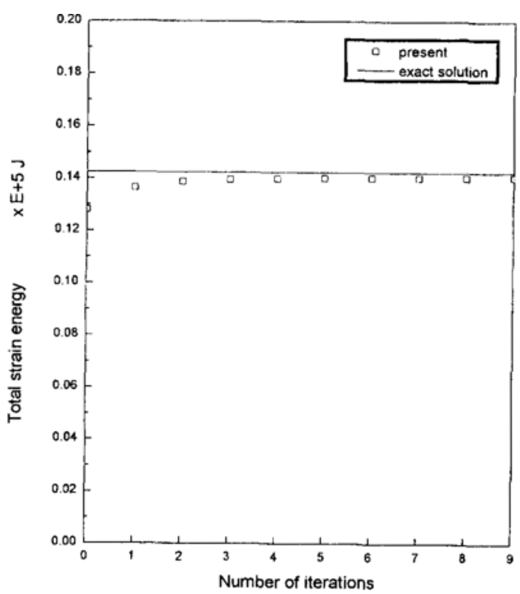

Fig. 8 Total strain energy vs. iteration numbers for the two-material cantilever beam ($E_1/E_2=0.01$).

Figure 5 shows that the total strain energy rapidly increases and converges to the exact result ($U_{total}=0.74210\text{E-1}$ MJ) in a few iterations.

When the moduli are reversed, similar observations are made. The variation of the stresses at the interface of two different materials along the beam is shown in Figs. 6 and 7. Comparison of the results of the conventional finite element analysis also reveals a very significant discontinuity between the computed stresses on the hard and soft sides of the interface. However, the present method yields nearly identical stresses in both materials at the interface. In addition, both stresses from the present method and the conventional finite element stresses on the soft side of the interface are in agreement with the exact results

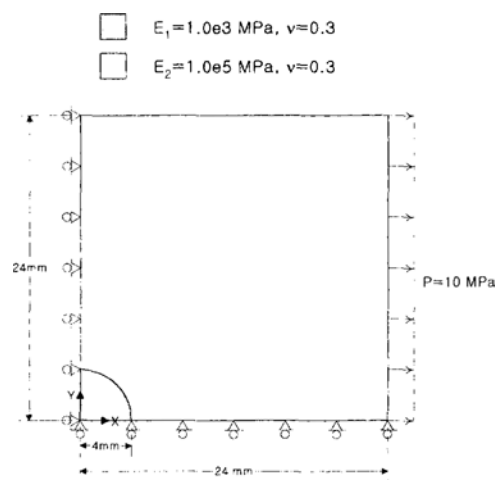

Fig. 9(a) A plate containing a circular disc of a different material under tension.

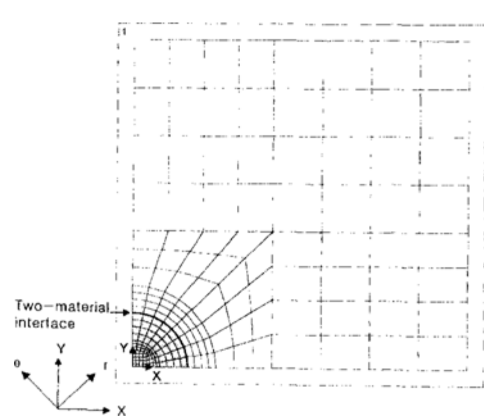

Fig. 9(b) Finite element model.

($\sigma_y=0$, $\tau_{xy}=0.0216345$ MPa) in every area except the region close to the fixed end. The variation in total strain energy versus number of iteration as shown in Fig. 8, shows that the total strain energy also rapidly increases and converges to the exact result ($U_{total}=0.14227E-1$ MJ) in a few iterations. Convergence of the total strain energy to the exact result, as shown in Figs. 5 and 8, denotes that the continuous stress field from the present method is rapidly improved as the iteration proceeds.

From Figs. 3, 4, 6, and 7, the stresses on the soft side of the two-material interface seem to be more reliable than the hard side. However, the fact that this observation is not true in general can be seen in the following example.

5.2 Example 2: Plate with circular inclusion of different material

Figure 9(a) shows a plate containing a circular disc made of a material 100 times softer than a plate and subjected to a uniform uniaxial tension at both its ends. Fig. 9(b) shows its finite element model with quadrilateral plane strain elements. Due to symmetry, one-quarter of the plate is taken for analysis, as shown in Fig. 9. The analytical solution for an infinite plate containing a circular disc of different material is available in the literature (Muskhelishvili, 1963). The size of the plate relative to the disc in Fig. 9 justifies the use of this closed-form analytical solution. Fig-

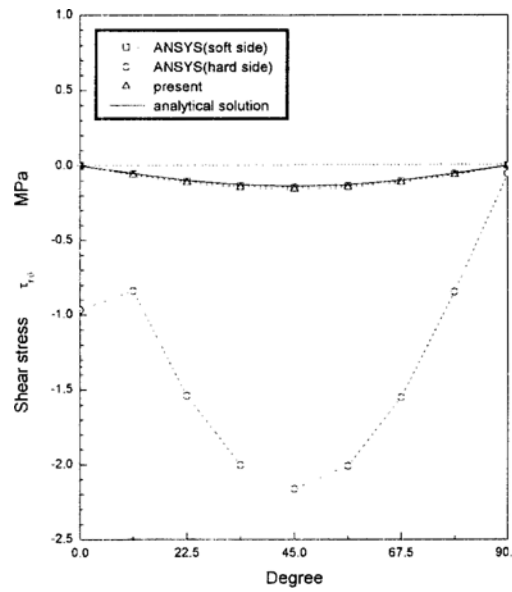

Fig. 11 Shear stresses at the two-material interface along the circumference (soft inclusion, $E_1/E_2=0.01$)

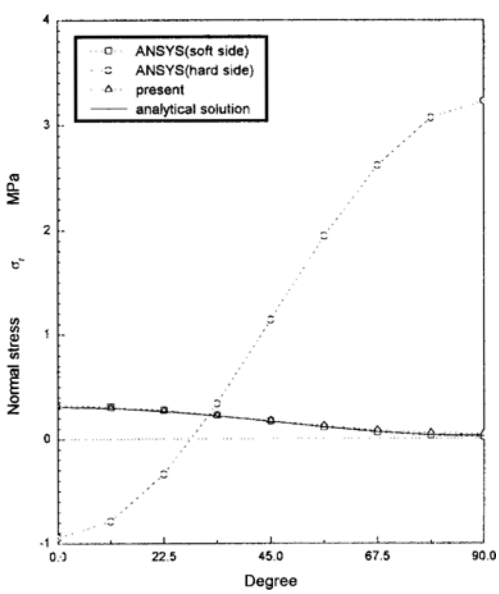

Fig. 10 Normal stresses at the two-material interface along the circumference (soft inclusion, $E_1/E_2=0.01$).

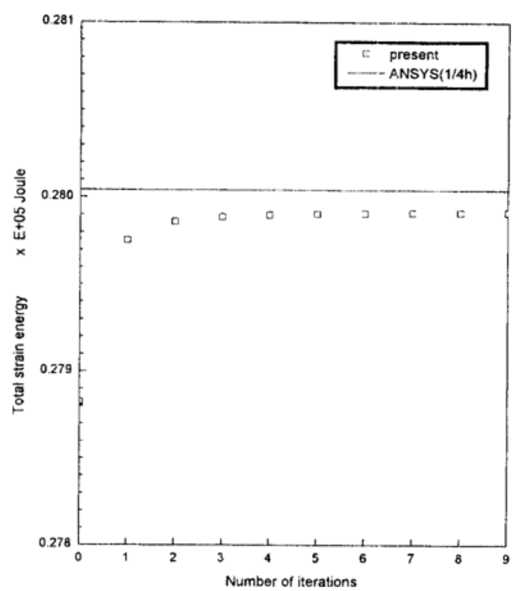

Fig. 12 Total strain energy vs. interation numbers for a plate containing a circular disc (soft inclusion, $E_1/E_2=0.01$)

ures 10 and 11 show the variation of stresses along the interface of two different materials for the conventional finite element solution, the present results and the closed-form analytical solution. Again, a very significant discontinuity is seen between the stresses by the conventional finite element method on the hard and soft sides of the interface. And the stresses from the present method are in agreement with the conventional finite element stresses on the soft side of the interface and the analytical solution. The variation of total strain energy versus number of iteration as shown in Fig. 12, shows that the total strain energy rapidly increases and converges to a somewhat smaller value than the assumed analytical solution from a refined mesh of $\frac{1}{4}h$ in a few iterations.

When the moduli are reversed, an interesting observation is made. The variation of the stresses at the interface of two different materials is shown in Figs. 13 and 14. Comparison of the results of the conventional finite element analysis also reveals a very significant discontinuity between the computed stresses on the hard and soft sides of the interface. In contrast to the previous analysis, however, the results on the hard side are closer to the exact solution than those on the soft side. The indication that the stresses on the softer side of a two-material interface are more reliable than those on the harder side is, therefore, not a gener-

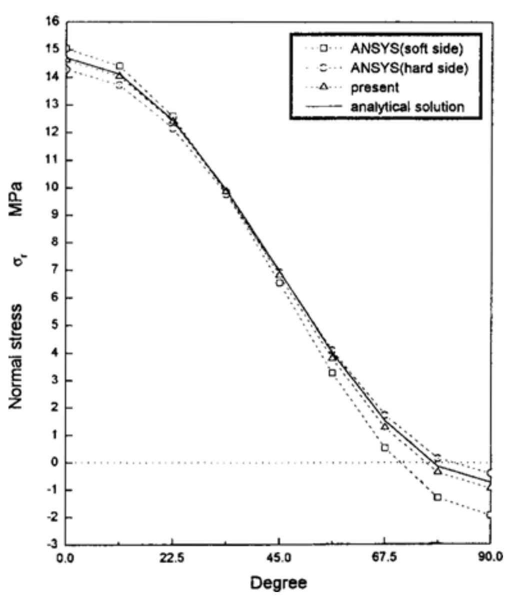

Fig. 13 Normal stresses at the two-material interface along the circumference (hard inclusion, $E_1/E_2=100$).

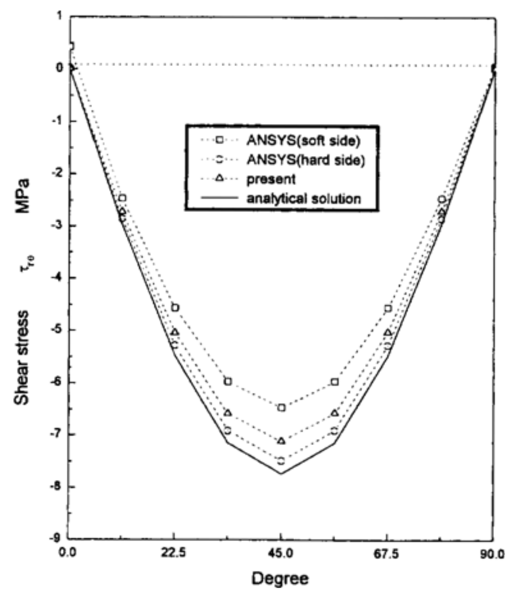

Fig. 14 Shear stresse at the two-material interface along the circumference (hard inclusion, $E_1/E_2=100$).

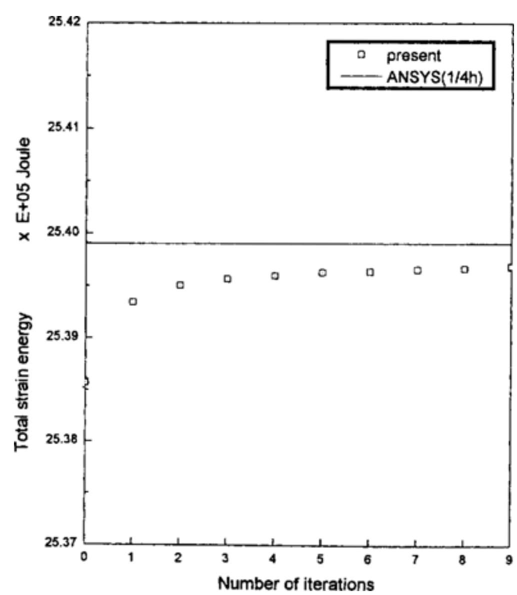

Fig. 15 Total strain energy vs. iteration numbers for a plate containing a circular disc (hard inclusion, $E_1/E_2=100$).

al one. The variation of total strain energy versus number of iteration as shown in Fig. 15, shows that the total strain energy also rapidly increases and converges to a somewhat smaller value than the assumed analytical solution from a refined mesh of $\frac{1}{4}h$ in a few iterations.

6. Conclusions

The initial displacement field and interfacial tractions are obtained by modifying the potential energy functional with a penalty function, which enforces the continuity of stresses at the interface of two different materials. The conventional projection method for stress smoothing is modified by imposing the interfacial tractions as the constraints. An iterative procedure to build a continuous stress field over the entire domain, including at the interface of dissimilar materials, is proposed by combining the modified projection method for stress-smoothing with the Loubignac-Cantin iteration for the restoration of momentum balance in smoothed stress fields. The proposed iterative procedure is used for stress analysis on two examples consisting of highly dissimilar materials, and the results are compared with those obtained from conventional finite element analysis and exact solutions. The proposed iterative procedure is performed satisfactorily in the test examples in a few iterations, and is therefore considered to be a reliable and cost-effective method to build an improved continuous stress field over the entire domain, including the interface of dissimilar materials. In contrast, the conventional displacement-based finite element formulation results in significantly discontinuous stresses at the interface of two different materials.

References

ANSYS User's *Manual for Revision 5.0, 1992,* Swanson Analysis System, Inc.

Brauchli, H. J. and Oden, J. T. , 1971, "Conjugate Approximation Function in Finite-element Analysis," *Quarterly of Applied Mathematics,* No. 1, April, pp. 65～90.

Chouchaoui, B. and Shirazi-Adl, A., 1992," A Mixed Finite Element Formulation for the Stress Analysis of Composite Structures," *Computers & Structures,* Vol. 43, No. 4, pp. 687～698.

Hinton, E. and Campbell, J. S., 1974, "Local and Global Smoothing of Discontinuous Finite Element Functions Using a Least Squares Method," *International Journal for Numerical Methods in Engineering,* Vol. 8, pp. 461～480.

Kim, D. S. and Lee, B. C., 1993, "Application of the Combined Mixed Functional to Finite Element Analysis of Bonding Problems," *Computational Engineering* (Edited by B. M. Kwak and M. Tanaka), ELSEVIER, AMSTERDAM, pp. 77～82.

Kim, Y. H., 1994, "Analysis of 2-D Bonding Problems Using Perturbed Lagrangian Method," M. S. Thesis, KAIST (in Korea).

Loubignac, G., Cantin, G., and Touzot, G., 1977, "Continuous Stress Field in Finite Element Analysis," *AIAA Journal,* Vol. 15, No. 11, pp. 1645～1646.

Muskhelishvili, N. I., 1963, *Some Basic Problems of Mathematical Theory of Elasticity* (*Translated by J. R. M. Radok*), pp. 205～229. pp. 641～649, Noordhoff, Groningen, Holland.

Shirazi-Adl, A., 1989, "An Interface Continuous Stress Penalty Formulation for the Finite Element Analysis of Composite Media," *Computers & Structures,* Vol. 33, No. 4, pp. 951～956.

Shirazi-Adl, A., 1992, "Finite Element Stress Analysis of a Push-out Test Part 1: Fixed Interface Using Stress Compatible Elements," *ASME Journal of Biomechanical Engineering,* Vol. 114, pp. 111～118.

Song, K. N., 1997, "A Study on the Improvement Method of the Stress Field Analysis in a Domain Composed of Dissimilar Materials," *Transactions of KSME* (*A*), Vol. 21, No. 11, pp. 1844～1851 (in Korea).

Zienkiewicz, O. C., Xi-Kui, Li, and Nakazawa, S., 1985, "Iterative Solution of Mixed Problems and the Stress Recovery Procedures," *Communications in Applied Numerical Method,* Vol. 1, pp. 3～9.

Zienkiewicz, O. C. and Zhu, J. Z., 1992, "The Superconvergent Patch Recovery and *a Posteriori* Error Estimates. Part 1: The Recovery Technique," *International Journal for Numerical Methods in Engineering,* Vol. 33, pp. 1331～1364.

Zienkiewicz, O. C., Vilotte, J. P., Toyoshima, S., and Nakazawa, S., 1985, "Iterative Method for Constrainted and Mixed Approximation. An Inexpensive Improvement of F. E. M Performance," *Computer Methods in Applied Mechanics and Engineering,* Vol. 51, pp. 3～29.